Pollution Characteristics and Sources of Carbon Components and Water-Soluble Ions in Atmospheric Particulate Matter in Nanjing, China

Wentao Yu, Maoyu Cao, Mindong Chen[*]

Jiangsu Key Laboratory of Atmospheric Environment Monitoring and Pollution Control, Collaborative Innovation Center of Atmospheric Environment and Equipment Technology, School of Environmental Science and Engineering, Nanjing University of Information Science & Technology, Nanjing, China

Email address:

yuwentao19@163.com (Wentao Yu), 20201248092@nuist.edu.cn (Maoyu Cao), chenmd@nuist.edu.cn (Mindong Chen)
[*]Corresponding author

Abstract: Nanjing, an important city in the Yangtze River Delta region, faces serious air pollution problems, especially particulate pollution. $PM_{2.5}$ can reduce atmospheric visibility and affect climate change, as well as adversely affect human health. Therefore, it is very necessary to monitor the components of $PM_{2.5}$. In order to study the component characteristics and sources of $PM_{2.5}$ in the northern suburbs of Nanjing, 191 $PM_{2.5}$ samples were collected and quantitatively analyzed for water-soluble ions (WSI), organic carbon (OC), elemental carbon (EC) and water-soluble organic carbon (WSOC). The annual average mass concentrations of OC, EC, and WSOC were 5.30 µg m^{-3}, 0.96 µg m^{-3}, and 3.09 µg m^{-3}, respectively. The variation characteristics of their seasonal abundance were basically the same, which reached the maximum in winter and the lowest in summer. Based on the ratio of organic carbon to elemental carbon, we find that the air in the northern suburbs of Nanjing is affected by coal burning, exhaust emissions and biomass combustion. The annual mean mass concentration of WSI in $PM_{2.5}$ was 23.00 µg m^{-3}, and the order of seasonal concentration was winter > autumn > spring > summer. The WSI in $PM_{2.5}$ are mainly SO_4^{2-}, NO_3^-, and NH_4^+. Through the concentration ratio of NO_3^-/SO_4^{2-}, we found that mobile sources were the main sources of pollution in autumn and winter, while stationary sources were the main sources of pollution in summer. Through the iterative calculation of PMF, five sources of $PM_{2.5}$ are determined, which are second generation (37.5%), traffic-related source (36.7%), combustion source (9.6%), marine source (8.5%), and industrial emissions (7.7%). In different seasons, $PM_{2.5}$ is significantly correlated with SO_4^{2-}, NO_3^-, and NH_4^+, indicating that $PM_{2.5}$ mainly comes from secondary generation.

Keywords: $PM_{2.5}$, Carbon Components, Water-Soluble Ions, Source Analysis

1. Introduction

In recent years, China often appears haze weathers, severe haze will reduce atmospheric visibility, affect climate change and even affect human health [1-4]. $PM_{2.5}$ was the main monitoring index, and secondary inorganic aerosols (SO_4^{2-}, NH_4^+, and NO_3^-), organic carbon (OC), elemental carbon (EC) and other trace organic compounds were the main components [5-7].

Carbon aerosol is an important part of atmospheric aerosol, accounting for 10-70% of $PM_{2.5}$ [8, 9]. It is mainly divided into organic carbon (OC), elemental carbon (EC) and inorganic carbon (IC) [1, 10]. OC is mainly generated from biomass and coal combustion, direct emissions from tail gas and industrial emissions, or through photochemical oxidation of organic gas [11]. The former is usually defined as primary organic carbon and the latter as secondary organic carbon according to the mode of source [9, 12]. It can also affect cloud condensation nuclei (CCN) which then impacts earth radiation balance and global climate change [13, 14]. When biomass and fossil fuels are burned incompletely, large amounts of EC are produced. Because of its good adsorption

activity, it can adsorb secondary pollutants and have a negative impact on the environment [15, 16].

Water-soluble ions (WSI), as important components, account for about 50% of $PM_{2.5}$ [17]. They are often used to identify the source of $PM_{2.5}$. For example, K^+ can be used as a tracer to evaluate biomass combustion; SO_4^{2-}, NH_4^+, and NO_3^- are related to secondary generation; high abundances of Na^+ and Cl^- are generally found in marine aerosols, which can be transported to coastal and inland areas due to air mass transport [18, 19]. Previous studies have shown that water-soluble ions are hygroscopic and can affect aerosol composition, size and pH [17, 20].

The Yangtze River Delta region, China's largest economic zone, has a large population and dense cities. This area is not only an important agricultural production base in China, but also a large number of chemical enterprises. A large number of gaseous pollutants are discharged in the process of industrial production and vehicle driving, which makes the air pollution situation increasingly serious and seriously affects people's health and daily life. The Yangtze River Delta is faced with serious air pollution due to a large number of human activities. As a megalopolis in the Yangtze River Delta region and the capital city of Jiangsu Province, Nanjing also faces serious air pollution problems. Therefore, it is necessary to monitor carbon components and water-soluble ions in the atmosphere of Nanjing.

Therefore, this study conducted one-year sampling in the northern suburbs of Nanjing from March 2017 to February 2018, and analyzed $PM_{2.5}$ samples by ion chromatography. The mass concentrations of five kinds of cations (Na^+, NH_4^+, K^+, Mg^{2+}, Ca^{2+}) and four kinds of anions (F^-, Cl^-, SO_4^{2-}, NO_3^-) were obtained, and the concentration level and correlation of water-soluble ions as well as the ratio of NO_3^-/SO_4^{2-} were analyzed. In order to comprehensively understand the pollution characteristics of $PM_{2.5}$ in the northern suburbs of Nanjing, the OC, EC and WSOC in the samples were measured by the elemental carbon organic carbon analyzer and total organic carbon analyzer, and the values of POC and SOC were estimated, so as to comprehensively understand the pollution characteristics and sources of carbon components in $PM_{2.5}$ in the northern suburbs of Nanjing.

2. Experimental Methods

2.1. Sampling Location and Time

The sampling site is set on the roof of the library of Nanjing University of Information Science and Technology (32°12′9′′N, 118°42′49′′E, Figure 1), about 20 m from the ground, located in the northern suburbs of Nanjing, 23 km from the urban area. There are no obstructing objects around him, so the air flows well. It is Jiangbei Avenue Expressway 1 km to the east, and the traffic flow is large. The sampling time is from March 2017 to February 2018, 24 hours continuous sampling from 12:00 to 12:00 the next day. The $PM_{2.5}$ large flow sampler (TISCH, USA) is used, and the flow rate is 1.13 m^3/min. The sampling period is mainly sunny and cloudy. In case of rain and snow, the sampler will be turned off. Periodically clean the sampler and calibrate the flow.

2.2. Sample Collection and Storage

The sampling membrane was quartz filter membrane (QM/A; Whatman; Middlesex, UK), 20.30 cm × 25.40 cm. Before sampling, the quartz filter membrane was placed in a Muffle furnace and roasted at 450°C for 4 h to remove residual organic matter, and then balanced in a constant temperature tank for 24 h. The quartz filter film before and after sampling was weighed by 1/100,000th electronic balance, which was weighed three times, and the average value of the three times was recorded as the weight of the filter film. The quality difference between quartz filter film before and after sampling is the quality of collected particles. After sample collection, the filter film was wrapped with tin foil and stored in a refrigerator at -20°C for subsequent sample analysis.

2.3. OC and EC Analysis

The OC and EC in the sample were determined by the elemental carbon organic carbon analyzer (Sunset Model, United States), which consists of organic carbon/elemental carbon analyzer host, vacuum pump and computer. Before injection and analysis, the filter membrane and blank filter membrane with a diameter of 17 mm collected $PM_{2.5}$ samples were cut with a punch. Also, the instrument should be turned on for an hour to stabilize and calibrated with a 99.9% sucrose solution. The main calibration uses sucrose solution, which can be used for online monitoring or offline monitoring, and can analyze and measure elemental carbon and organic carbon at the same time. Its detection limit was 0.2 $\mu g/cm^2$ and the detection range was 0.2-1000 $\mu g/cm^2$. In addition, during the determination of aerosol samples, a blank sample analysis was performed for every ten samples.

2.4. Water-Soluble Inorganic Ions Analysis

Anions (F^-, Cl^-, NO_3^-, SO_4^{2-}) were analyzed by using the Ion chromatograph (ICS-2000) produced by Diane Company in the United States, and cations (NH_4^+, Ca^{2+}, Na^+, Mg^{2+}, K^+) were analyzed by using the ion chromatograph (ICS-3000). First analyze the standard sample solution prepared with chromatographically pure pharmaceutical grade, then create a standard curve, and finally inject the sample for analysis. The sample pretreatment steps are: take a filter membrane with a diameter of 3.6 cm, cut it into pieces with ceramic scissors, put it into a 50 mL centrifuge tube, add 45 mL of ultrapure water, tighten the cap, seal it with tin foil, and add an ice pack for sonication. Extraction was carried out for 60 min, during which the water temperature could not exceed 20°C. After sonication, a 0.22 μm PTFE syringe-type microporous membrane was used to filter the samples for analysis. The correlation coefficient of the configured standard curve is above 0.999. In order to reduce the error of the blank sample and make the result more reliable, a blank control experiment is set up. Quantitative standard solution was added to two blank samples and five tested samples. The recoveries were all

between 90% and 110% after instrument determination.

2.5. WSOC Analysis

The total organic carbon/total nitrogen analyzer (TOC/TN instrument, TOC-L type, Shimadzu Corporation, Japan) was used to analyze the content of WSOC in the sample, and the oxidative combustion infrared analysis method was used to measure the Total carbon (TC) and Inorganic carbon (IC), the value of WSOC is obtained by subtracting the two. The operation was as follows: 3.6 cm diameter sample filter membrane and blank filter membrane were cut with a hole punch, 45 mL ultrapure water was added, ultrasonic extraction was carried out for 3 times, 20 minutes each time, then filtration was carried out, and finally 30 mL sample was taken for analysis. Before WSOC analysis, ensure that the correlation coefficient required by the standard curve reaches 99.9%, and analyze 30 mL of ultrapure water before analyzing the atmospheric sample, and do blank sample analysis for every ten samples.
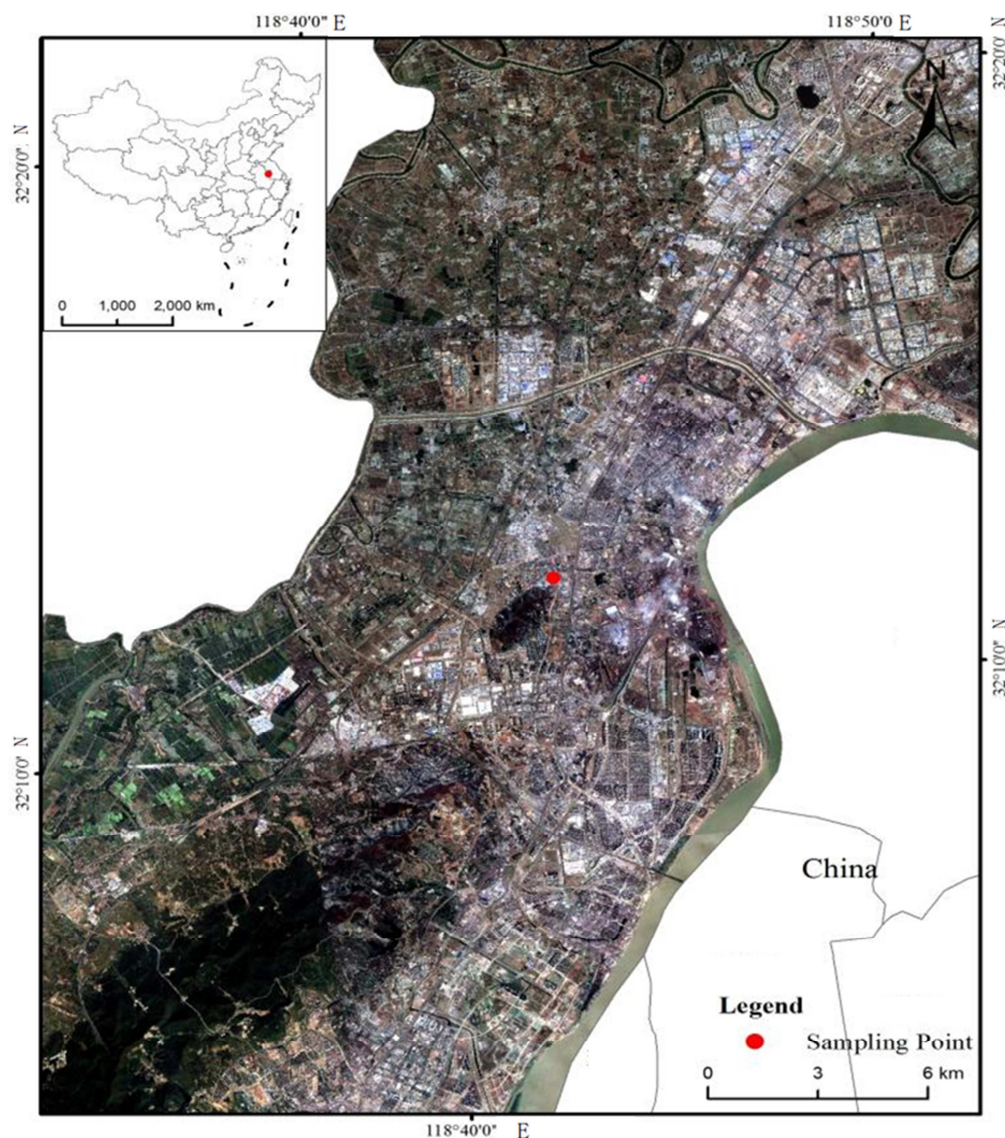

Figure 1. *The location of sampling site.*

2.6. Data Analysis

SPSS software was used to analyze the correlation between carbon components, water-soluble ions and $PM_{2.5}$, so as to further explore the source of $PM_{2.5}$.

In this study, OC, EC and water-soluble ions were used to determine the source of $PM_{2.5}$. A detailed description of the PMF software and a user's guide can be found on this website: www.epa.gov/air-research/positive-matrix-factorizationmodel-environmental-data-analyes. Two data files are required to run the PMF model: concentration files and uncertainty files. The error rate was set at 15%. For the uncertainty value, if the concentration is less than or equal to the method detection limit:

$$Unc = 5/6MDL$$

If the concentration is greater than the method detection limit:

$$Unc = \sqrt{(ErrorFraction + concentration)^2 + (0.5 \times MDL)^2}$$

3. Results and Discussion

3.1. Ambient Concentrations of Carbonaceous Aerosols in PM$_{2.5}$ During 2017

3.1.1. Overview of Carbon Components Concentrations

The concentrations of OC, EC and WSOC in atmospheric PM$_{2.5}$ samples from the northern suburbs of Nanjing were obtained, as well as the mean, maximum and minimum values of each season from March 2017 to February 2018. Total carbon aerosol (TCA) can be estimated by the mass concentration of OC and EC, the specific formula is

TCA=1.6×OC+EC.

As can be seen from Table 1, the average concentrations of OC, EC and WSOC in PM$_{2.5}$ in the northern suburbs of Nanjing in 2017 were 5.30 µg m^{-3}, 0.96 µg m^{-3}, and 3.09 µg m^{-3}, respectively. The maximum value of OC (20.71 µg m^{-3}) appeared on November 23, while the minimum value (1.08 µg m^{-3}) appeared on October 17. The maximum peak value of EC (3.46 µg m^{-3}) also occurred on October 17, but the minimum peak value (0.22 µg m^{-3}) occurred on October 15. It could be seen from Table 1 that the annual average mass concentration of TCA was 9.31 µg m^{-3}. The maximum concentration was 36.6 µg m^{-3} on November 23 in autumn, which was consistent with the maximum value of OC and EC. The minimum value also appeared in autumn, and the mass concentration was 1.96 µg m^{-3}.

Table 1. *The concentrations of carbon components and water-soluble ions of PM$_{2.5}$ in Nanjing, 2017.*

Components	Concentrations (µg m^{-3})				
	Annual	Spring (n=37)	Summer (n=53)	Autumn (n=60)	Winter (n=41)
Na$^+$	0.99 (0.46-1.94)	0.67 (0.48-1.08)	1.20 (0.91-1.71)	0.97 (0.46-1.94)	1.02 (0.48-1.66)
NH$_4^+$	4.39 (0.57-16.67)	3.10 (0.77-8.48)	2.25 (0.57-6.91)	4.72 (0.58-11.72)	7.85 (2.20-16.67)
K$^+$	0.75 (0.33-2.60)	0.74 (0.38-3.80)	0.51 (0.33-0.85)	0.79 (0.33-2.60)	1.02 (0.44-2.08)
Mg^{2+}	0.35 (0.26-0.83)	0.37 (0.28-0.83)	0.33 (0.26-0.43)	0.34 (0.27-0.48)	0.36 (0.27-0.46)
Ca^{2+}	1.36 (0.37-4.53)	1.75 (0.37-4.53)	0.99 (0.64-1.92)	1.24 (0.46-4.11)	1.67 (0.60-3.60)
F$^-$	0.06 (0.01-0.34)	0.04 (0.01-0.19)	0.04 (0.01-0.07)	0.05 (0.01-0.16)	0.12 (0.01-0.34)
Cl$^-$	0.95 (0.08-7.02)	0.66 (0.17-2.52)	0.32 (0.11-7.02)	0.74 (0.08-2.22)	2.33 (0.60-3.60)
SO$_4^{2-}$	6.68 (0.03-20.82)	5.67 (1.79-11.22)	6.06 (0.29-20.82)	6.99 (1.77-14.28)	7.92 (0.03-0.34)
NO$_3^-$	7.47 (0.25-21.23)	5.58 (0.80-19.07)	2.37 (0.45-6.22)	8.23 (0.51-21.23)	14.68 (0.25-5.45)
NO$_3^-$/ SO$_4^{2-}$	1.18 (0.04-15.00)	1.00 (0.17-1.42)	0.70 (0.04-15.00)	1.19 (0.22-0.57)	1.97 (0.81-5.37)
OC	5.30 (1.08-20.71)	6.45 (1.77-16.95)	3.47 (1.30-6.05)	4.42 (1.08-20.71)	8.29 (2.59-18.33)
EC	0.96 (0.22-3.64)	0.68 (0.28-2.47)	0.70 (0.22-3.46)	1.18 (0.45-2.57)	0.84 (0.22-3.64)
TCA	9.31 (1.96-36.60)	11.28 (3.36-30.7)	6.23 (2.36-12.11)	7.77 (1.96-36.60)	14.43 (4.87-31.1)

Table 2 shows the comparison of the mass concentrations and ratios of OC and EC in the atmospheric PM$_{2.5}$ in the northern suburbs of Nanjing and others cities. It can be seen that compared with the northern cities such as Handan and Beijing, the atmospheric concentration level of OC and EC in Nanjing is lower. Among them, the mass concentrations of OC and EC in Handan were higher than those in major cities in China, which were 3 times and 10 times higher than those in the northern suburbs of Nanjing in this study, respectively. This may be due to the industrial structure of resource-based heavy industry in the region and the use of coal for heating in winter. The concentrations of OC and EC in the Shanghai area were significantly higher than those in the inland areas, which may be caused by the oceanic airflow. The mass concentration of OC in Shanghai is slightly higher than that of this sampling point, and the mass concentration of EC is about 3.5 times that of this sampling point, and the source of EC is related to vehicle exhaust emissions [21]. This may be due to the developed traffic in Shanghai and the large number of motor vehicles, resulting in increased exhaust emissions.

3.1.2. Seasonal Characteristics of Carbon Components

In the northern suburbs of Nanjing, the concentration of OC was the highest in winter (8.29 µg m^{-3}), followed by spring (6.45 µg m^{-3}) and autumn (4.42 µg m^{-3}), and the lowest in

summer (3.47 µg m^{-3}). The average mass concentration of OC in winter was 2.4 times that of summer. OC showed obvious seasonal variation, which may be closely related to seasonal climate change. Because the sampling site is close to the industrial zone, there is a large number of industrial combustion phenomenon, and residents also burn wood for heating. In winter, the mixed layer height is low, and PM$_{2.5}$ tends to gather to a higher concentration, resulting in the highest OC concentration in winter. The average mass concentration of OC was the lowest in summer, which may be due to the influence of East Asian monsoon in Nanjing, which resulted in more atmospheric precipitation, which was conducive to the diffusion and removal of pollutants.

The average mass concentration of EC in PM$_{2.5}$ in spring, summer, autumn and winter were 0.96 µg m^{-3}, 0.68 µg m^{-3}, 0.70 µg m^{-3}, and 1.18 µg m^{-3}, respectively. It can be seen that the average mass concentration of EC is the highest in winter and the lowest in summer, of which the average mass concentration of EC in winter is 1.7 times that in summer. This may be due to the fact that the sampling site is close to Jiangbei Expressway, and the large traffic flow in winter leads to larger automobile exhaust emissions. In addition, under cold meteorological conditions, it is not conducive to the diffusion of pollutants, so the concentration of EC is higher in winter. In contrast, the average mass concentration of EC in

summer is the lowest, which may be because of more rainfall in summer, which can remove pollutants in the atmosphere to some extent. The seasonal variation trend of TCA and WSOC was the same as that of OC and EC, with the highest average mass concentration in winter and the lowest in summer. In addition, the average mass concentration of TCA in winter was 4.2 times that in summer.

Table 2. *Comparison of OC and EC concentrations ($\mu g\ m^{-3}$) measured in worldwide.*

Sampling locations	Sampling date	PM$_{2.5}$ ($\mu g\ m^{-3}$)	OC ($\mu g\ m^{-3}$)	EC ($\mu g\ m^{-3}$)	OC/EC	Reference
Nanjing	March 2017-February 2018	84.08	5.30	0.84	6.80	In this study
Handan, China	2017	101.88	25.16	2.87	10.33	[16]
Mount Tai, North China	June 2015-August 2015	-	4.42	1.58	2.98	[9]
Beijing, China	Jul 2012-Apr 2013	95.6	13.3	3.3	3.7	[10]
Shanghai, China	October 2011-August 2012	90.3	7.6	2.9	2.8	[22]
Chongqing, China	November 2019-October 2020	38.50	9.03	2.45	-	[23]
Inchon, Korea	Jun 2009–May 2010	-	41.9	10.9	1.8	[24]
Madrid, Spain	Feb 2006–Jun 2008	-	3.7	1.3	4.3	[12]
Western Taiwan Strait Region	November 2010, January, April and August 2011	-	12.7	2.3	5.8	[25]

3.1.3. OC/EC

OC/EC ratio is not only related to the source of carbon aerosols, but also can be used to judge the existence of secondary organic aerosols [26]. If the ratio of OC/EC is greater than 2, it indicates the presence of SOC in the atmosphere [27]. As can be seen from Table 3, the average annual ratio of OC/EC in PM$_{2.5}$ in the northern suburbs of Nanjing in this study is 6.79, and the ratios of OC/EC in spring, summer, autumn and winter are 7.65, 5.71, 6.67 and 7.74, respectively. Compared with major cities in China, the OC/EC ratio in the northern suburbs of Nanjing is higher than that in Beijing and Shanghai (Table 2).

Table 3. *The concentrations of SOC, POC and OC/EC ratio in different seasons.*

	OC/EC	SOC ($\mu g\ m^{-3}$)	POC ($\mu g\ m^{-3}$)	SOC/OC	POC/OC	WSOC ($\mu g\ m^{-3}$)
Spring	7.65	3.72	2.73	57.20%	42.80%	2.85
Summer	5.71	2.26	1.21	64.99%	35.01%	2.25
Autumn	6.67	2.62	1.80	55.54%	44.46%	3.07
Winter	7.74	4.67	3.62	55.88%	44.12%	4.56
Annual	6.79	3.13	2.16	58.76%	41.24%	3.09

Studies have shown that the OC/EC ratio of gasoline and diesel vehicle exhaust is 1.0-4.2, and the OC/EC ratio of coal is 2.5-10.5. In addition, the OC/EC ratio is between 8.1-12.7, indicating the existence of biomass combustion emissions. As can be seen from Table 3, during the sampling period, the annual mean value of OC/EC in the northern suburbs of Nanjing was 6.79. The ratio of OC/EC in spring, summer, autumn and winter was 7.65, 5.71, 6.67 and 7.74, respectively, with the highest value in winter, followed by spring and autumn, and the lowest value in summer. In addition, the minimum OC/EC ratio was 1.79 and the maximum was 12.92 in the whole year. Therefore, Nanjing may be affected by vehicle exhaust, coal burning and biomass combustion.

3.1.4. SOC Estimation

OC includes primary organic carbon (POC) and secondary organic carbon (SOC). SOC is mainly generated by the photochemical reaction of volatile organic compounds (VOCs) in the atmosphere. In this study, the following formula is used to calculate SOC and POC [28]:

$$SOC = OC - POC$$

$$POC = EC \times (OC/EC)_{min}$$

Where, $(OC/EC)_{min}$ is the minimum value of OC/EC during the sampling period. Table 3 shows that the annual mean concentration of POC is 2.16 $\mu g\ m^{-3}$. The average concentration of POC was 3.62 $\mu g\ m^{-3}$, 2.73 $\mu g\ m^{-3}$, 1.80 $\mu g\ m^{-3}$, and 1.21 $\mu g\ m^{-3}$ in the four seasons from high to low, which was consistent with the seasonal trend of EC. In addition, the annual average proportion of POC in OC was 41.24%, less than 50%, indicating that OC was less affected by direct discharge of pollution sources. As can be seen from Table 3, the annual average mass concentration of SOC is 3.13 $\mu g\ m^{-3}$, and the average mass concentration in spring, summer, autumn and winter is 3.72 $\mu g\ m^{-3}$, 2.26 $\mu g\ m^{-3}$, 2.62 $\mu g\ m^{-3}$, and 4.67 $\mu g\ m^{-3}$, respectively. Meanwhile, the annual average SOC/OC ratio was 58.76%, and the SOC/OC ratio was 57.20%, 64.99%, 55.54%, and 55.88% in spring, summer, autumn and winter, respectively. The concentration of SOC was the highest in winter, about twice that in summer. This may be because the atmosphere is relatively stable in winter, which is not conducive to the diffusion of pollutants, and because of the increase of coal and biomass burning for winter heating, which leads to the highest concentration of SOC in winter. In summer, Nanjing is affected by monsoon, and precipitation weather increases. Precipitation can play a certain role in cleaning suspended particulate matter and gaseous pollution in the atmosphere, so the concentration of SOC in summer is the lowest.

3.2. Ambient Concentrations of Water-Soluble Ions in PM$_{2.5}$ During 2017

3.2.1. Overall Pollution Levels of Water-Soluble Ions

In this study, PM$_{2.5}$ samples were collected in the northern suburbs of Nanjing from March 2017 to February 2018, and WSI was measured and analyzed. The annual average mass concentration of total water-soluble ions is 23.00 μg m^{-3}, the minimum value is 5.55 μg m^{-3} in autumn, and the maximum value is 71.52 μg m^{-3} in winter. It can be found that during the

sampling period from February 2017 to March 2018, the maximum value of total water-soluble ions was 12.8 times the minimum value, indicating that the mass concentration of water-soluble ions in the atmospheric PM$_{2.5}$ in the northern suburbs of Nanjing changed greatly. The annual average mass concentration of WSI is in the order of NO$_3^-$ > SO$_4^{2-}$ > NH$_4^+$ > Ca^{2+} > Na$^+$ > Cl$^-$ > K$^+$ > Mg^{2+} > F$^-$. The average mass concentrations were 7.47 μg m^{-3}, 6.68 μg m^{-3}, 4.39 μg m^{-3}, 1.36 μg m^{-3}, 0.99 μg m^{-3}, 0.95 μg m^{-3}, 0.75 μg m^{-3}, 0.35 μg m^{-3}, and 0.06 μg m^{-3}, respectively.
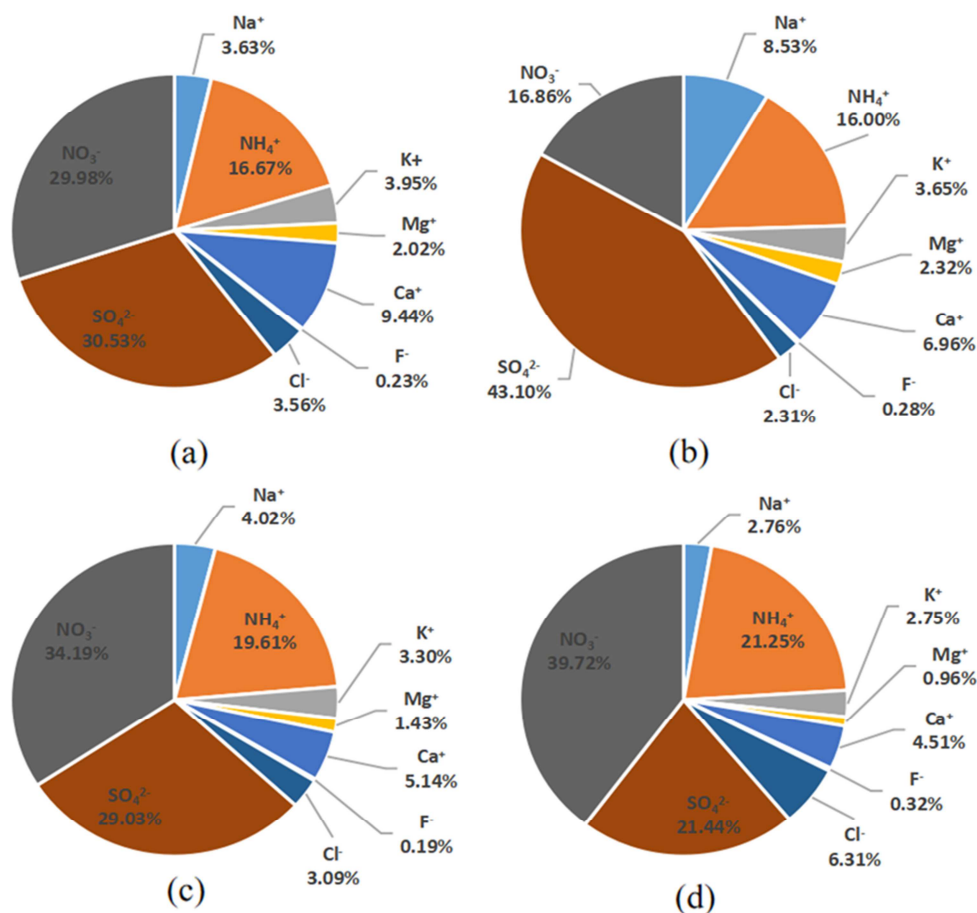

Figure 2. *The proportion of water-soluble ions in different seasons. (a) spring, (b) summer, (c) autumn, (d) winter.*

3.2.2. Seasonal Characteristics of Water-Soluble Ions

The average mass concentrations of WSI in PM$_{2.5}$ in the northern suburbs of Nanjing in spring, summer, autumn and winter were 18.60 μg m^{-3}, 14.06 μg m^{-3}, 24.08 μg m^{-3}, and 36.95 μg m^{-3}, respectively. In terms of seasons, the mass concentration of WSI was the highest in winter, and decreased in order of autumn, spring and summer. It can be seen from Figure 2 that the proportion of WSI is arranged in different order in each season. The proportion of different ions to total ions in spring is SO$_4^{2-}$ > NO$_3^-$ > NH$_4^+$ > Ca^{2+} > K$^+$ > Na$^+$ > Cl$^-$ > Mg^{2+} > F$^-$. The proportion of WSI in summer is SO$_4^{2-}$ > NO$_3^-$ > NH$_4^+$ > Na$^+$ > Ca^{2+} > K$^+$ > Mg^{2+} > Cl$^-$ > F$^-$. The ratio of Na$^+$ was higher in summer than in spring. The proportion of WSI in autumn is in the order of NO$_3^-$ > SO$_4^{2-}$ > NH$_4^+$ > Ca^{2+} > Na$^+$ > K$^+$ > Cl$^-$ > Mg^{2+} > F$^-$. The proportion of different ions to total

ions in winter is NO^{3-} > SO$_4^{2-}$ > NH$_4^+$ > Cl$^-$ > Ca^{2+} > Na$^+$ > K$^+$ > F$^-$. It can be seen that although the contributions of different ions are different in the four seasons, secondary inorganic ions (SO$_4^{2-}$, NO$_3^-$, and NH$_4^+$) occupy more than 70% of all ions in any season, which further indicates that secondary pollution occurs in the northern suburbs of Nanjing.

3.2.3. Ratio Analysis of NO$_3^-$/SO$_4^{2-}$

At present, the mass concentration ratio of NO$_3^-$/SO$_4^{2-}$ is used to judge the contribution of mobile sources and fixed sources to relative atmospheric pollution. If the mass concentration ratio of NO$_3^-$/SO$_4^{2-}$ is greater than 1, it indicates that the contribution of mobile sources is greater; if the mass concentration ratio of NO$_3^-$/SO$_4^{2-}$ is less than 1, it indicates that the contribution of fixed sources is greater [29]. From Table 1, NO$_3^-$/SO$_4^{2-}$-ratios in all seasons and throughout the

year, it can be concluded that the annual average NO_3^-/SO_4^{2-} ratio in $PM_{2.5}$ in the northern suburbs of Nanjing is 1.18. The average NO_3^-/SO_4^{2-} ratios in autumn and winter are all greater than 1, which are 1.19 and 1.97, respectively. This indicates that the contribution of mobile sources is greater than that of fixed sources in autumn and winter. Mobile sources are the main source of pollution, and mobile source pollution in winter is more serious than that in autumn. In summer, the average NO_3^-/SO_4^{2-} ratio is less than 1, indicating that the contribution of mobile sources is smaller than that of fixed sources in summer, and fixed sources are the main sources of pollution.

3.3. Possible Sources of $PM_{2.5}$

3.3.1. PMF Analysis

Using EPA PMF5.0 model and obtained data (191 samples × 11 species), the source contribution of $PM_{2.5}$ was explored. The exploration of PMF optimal scheme is determined by the number of factors of the change scheme. We simulated the schemes with 4-6 factors in turn, and each scheme was run and calculated 20 times. Finally, the scheme of 5 factors is determined as the best scheme, because it has more physical significance than others. Their source profiles and percentage contributions are depicted in Figure 3.
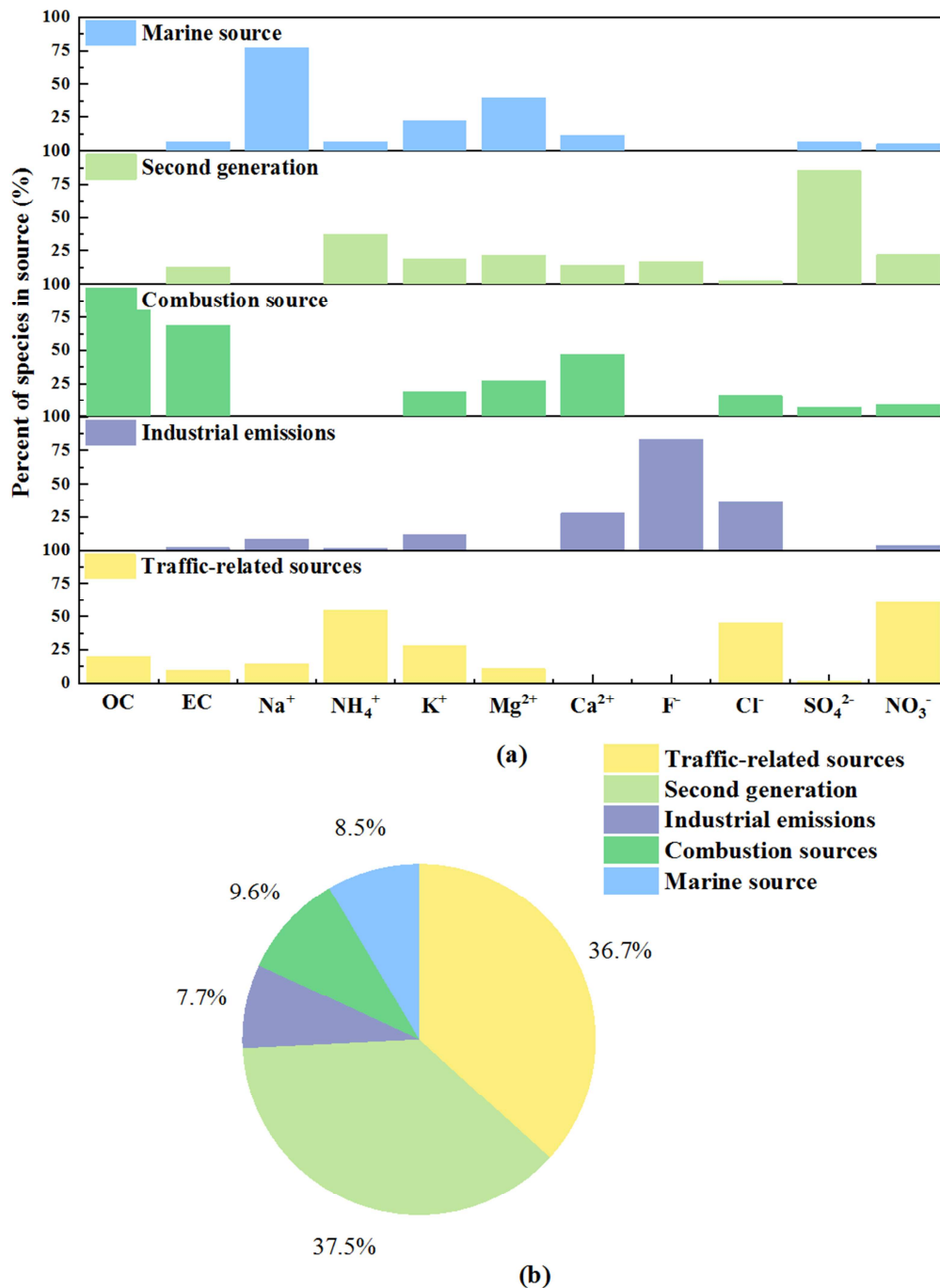

Figure 3. (a) The profile of each factor by PMF analyses. (b) The source contribution of the five factors to the total components in $PM_{2.5}$ of Nanjing in 2019.

We can see from Figure 3(a) that Na^+ (77.3%) has a high proportion in factor 1, and high abundances of Na^+ is generally found in marine aerosols. So factor 1 is defined as marine source. Factor 2 is defined as secondary generation, in which the contribution ratio of SO_4^{2-} (85.3%), NH_4^+ (37.5%), and NO_3^- (22%) is higher, and these ions are related to secondary generation. The proportion of OC and EC in factor 3 was 79.8% and 68.9%, respectively. In addition, Ca^{2+} (46.9%) also made certain contribution. Because OC and EC mostly come from biomass combustion and coal combustion, factor 4 is defined as the combustion source. Factor 4 is characterized by a high proportion of contributions from F^- (83.2%), Cl^- (36.2%), and Ca^{2+} (27.8%), which may come from industrial emissions. Factor 5 is defined as a traffic-related source, because NO_3^- (60.8%) and NH_4^+ (54.5%) have high contributions in this factor, because the exhaust emissions of vehicles such as cars will release pollutants such as nitrogen oxides. Figure 3(b) presents the contributions of five sources to mass $PM_{2.5}$, where second generation, traffic-related source, combustion sources, marine source, and industrial emissions are seen to account for 37.5%, 36.7%, 9.6%, 8.5%, and 7.7% of the total $PM_{2.5}$ mass in the suburban region. In Nanjing, secondary generation and traffic emissions are the main sources of $PM_{2.5}$ pollution, which together contribute 74.2%.

3.3.2. The Dominant Sources of $PM_{2.5}$ in Different Seasons

In order to better understand the dominant sources of $PM_{2.5}$ in different seasons, we conducted correlation analysis between $PM_{2.5}$ and characteristic components. It can be seen from Figure 4 that $PM_{2.5}$ has a good correlation with Ca^{2+} ($r=0.670$, $p<0.01$), Cl^- ($r=0.666$, $p<0.01$), and F^- ($r=0.657$, $p<0.01$), which means that most of $PM_{2.5}$ in Nanjing in spring may come from industrial emissions. At the same time,

secondary ions (SO_4^{2-}, NH_4^+, and NO_3^-) also show a good correlation with $PM_{2.5}$, and the contribution of secondary generation to $PM_{2.5}$ can not be ignored. The correlation between NH_4^+ and NO_3^- was the highest with a correlation coefficient of 0.895, followed by NO_3^- and Cl^- with a correlation coefficient of 0.668. NH_4^+ is likely to exist in the form of NH_4NO_3, NH_4Cl, and $(NH_4)_2SO_4$. It can be seen from Figure 4 that $PM_{2.5}$ is significantly correlated with NO_3^-, SO_4^{2-}, and NH_4^+ at 0.01 level, with correlation coefficients of 0.460, 0.499, and 0.590, respectively, indicating that $PM_{2.5}$ and SNA (NO_3^-, SO_4^{2-}, and NH_4^+) have the same source in summer. NH_4^+ was significantly correlated with SO_4^{2-} and NO_3^-, with correlation coefficients of 0.830 and 0.452, respectively. NH_4^+ may exist in the form of NH_4NO_3 and $(NH_4)_2SO_4$. In addition, $PM_{2.5}$ has a certain correlation with K^+ ($r=0.448$, $p<0.01$) and Ca^{2+} ($r=0.342$, $p<0.05$). This means that there may be biomass burning during the season because K^+ is a tracer of biomass burning. As can be seen from Figure 4, $PM_{2.5}$ is significantly correlated with K^+, SO_4^{2-}, NO_3^-, NH_4^+, and Ca^{2+} at the level of 0.01, with correlation coefficients of 0.566, 0.602, 0.658, 0.620, and 0.566, respectively. Different from summer, the correlation between $PM_{2.5}$ and K^+, Ca^{2+}, and Mg^{2+} increased in autumn, but the correlation between $PM_{2.5}$ and SNA did not change significantly. K^+ generally comes from biomass combustion, while Ca^{2+} and Mg^{2+} come from natural sources such as road dust and soil, indicating that the influence of biomass combustion and natural sources is greater in autumn than in summer. In winter, $PM_{2.5}$ is significantly correlated with SO_4^{2-}, NO_3^-, and NH_4^+ at 0.01 level, with correlation coefficients of 0.556, 0.566 and 0.637, respectively. Unlike in other seasons, there is no good correlation between other ions and $PM_{2.5}$, which means that $PM_{2.5}$ mainly comes from secondary generation in this season.
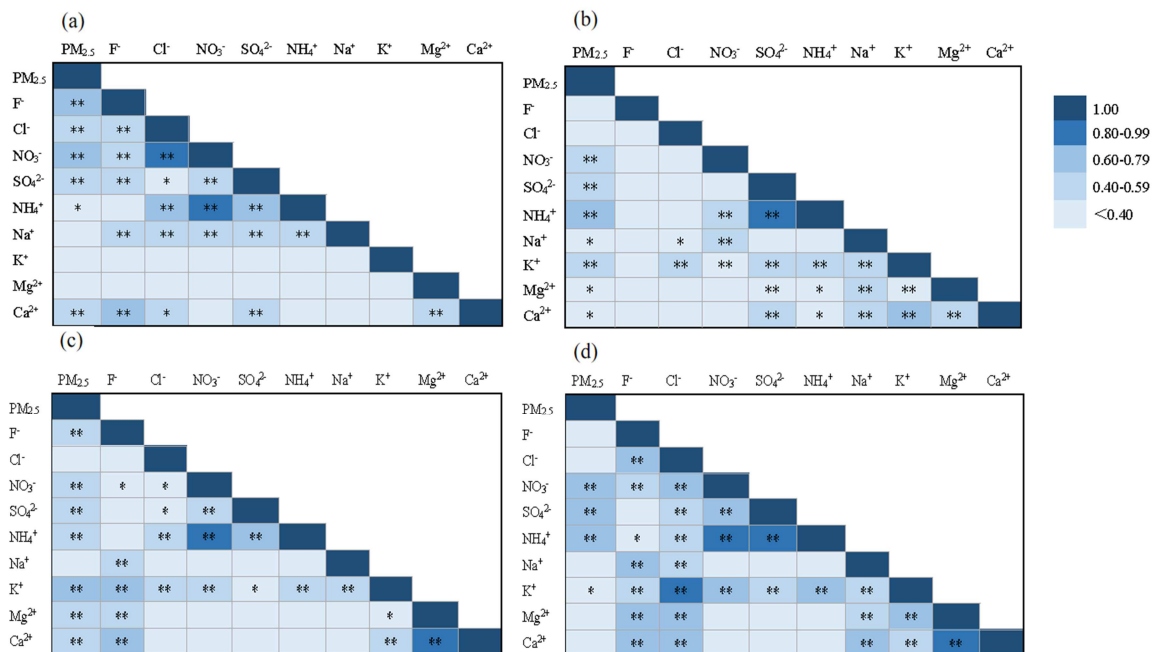

Figure 4. The correlation between $PM_{2.5}$ and its water-soluble ions in different seasons. (a) spring, (b) summer, (c) autumn, (d) winter.

4. Conclusion

In this study, carbon components (OC, EC, WSOC) and water-soluble ions in 191 $PM_{2.5}$ samples were determined. In the $PM_{2.5}$ samples collected in 2017, the average concentration of total carbon aerosol (TCA) was 9.31 μg m^{-3}, and the average concentration of OC and EC were 5.30 and 0.96, respectively. The concentrations of OC and EC in Nanjing were lower than those in North China, but similar to those in Shanghai. This may be due to the industrial structure of resource-based heavy industries in North China and the use of coal for heating in winter. All carbon components have obvious seasonal variation characteristics, that is, the highest abundance in winter and the lowest in summer. The dominant carbon components in the other three seasons were different, which might be due to the different source contributions of different components. OC/EC ratios in different seasons were used to explore the source of $PM_{2.5}$ in Nanjing, and it was found that may be affected by automobile exhaust, coal burning and biomass combustion.

The annual average mass concentration of WSI in $PM_{2.5}$ was 23.00 μg m^{-3}, and the average mass concentration of WSI in spring, summer, autumn and winter were 18.60 μg m^{-3}, 14.06 μg m^{-3}, 24.08 μg m^{-3} and 36.95 μg m^{-3}, respectively. The WSI in $PM_{2.5}$ are mainly SNA, which account for 80.62% of the total WSI. According to the analysis of NO_3^-/SO_4^{2-} mass concentration ratio, the results show that mobile source is the main source of pollution in autumn and winter, and fixed source is the main source of pollution in summer. In order to further understand the source of $PM_{2.5}$, the data of OC, EC and WSI were poured into PMF model to identify the source of $PM_{2.5}$. PMF results show that $PM_{2.5}$ mainly comes from five sources, namely transport-related sources, secondary generation, combustion sources, marine source, and industrial emissions, with contribution rates of 37.5%, 36.7%, 9.6%, 8.5%, and 7.7%, respectively. The correlation between $PM_{2.5}$ and ions is used to judge the source of advantage in different seasons. $PM_{2.5}$ was significantly correlated with SNA in different seasons, especially in autumn. Therefore, secondary generation was the main source of $PM_{2.5}$ in the northern suburbs of Nanjing in 2017.

5. Recommendations

This study has determined the conventional components in $PM_{2.5}$ and provided some information for air pollution research. In this study, it can be seen that carbonaceous component is an important component of $PM_{2.5}$, and the pollution characteristics of carbonaceous aerosols can be more comprehensively explored in future work. In particular, the contribution of organics (nitroaromatic acids, humic acids) to the light absorption of carbonaceous aerosols can be further investigated. In addition, this study shows that the secondary generation is an important source of air pollution in Nanjing, so it is very meaningful to carry out research on secondary aerosols, such as the concentration characteristics of secondary aerosols, generation mechanism, and source analysis.

Acknowledgements

References

[1] H. Yang, J. Wang, M. Chen, D. Nie, F. Shen, Y. Lei, P. Ge, T. Gu, X. Gai, X. Huang, Q. Ma, (2020) Chemical characteristics, sources and evolution processes of fine particles in Lin'an, Yangtze River Delta, China, Chemosphere, 254, 126851. doi: 10.1016/j.chemosphere.2020.126851.

[2] B. Ostro, B. Malig, R. Broadwin, R. Basu, E. B. Gold, J. T. Bromberger, C. Derby, S. Feinstein, G. A. Greendale, E. A. Jackson, H. M. Kravitz, K. A. Matthews, B. Sternfeld, K. Tomey, R. R. Green, R. Green, (2014). Chronic $PM_{2.5}$ exposure and inflammation: Determining sensitive subgroups in mid-life women, Environmental Research, 132 168-175. doi: 10.1016/j.envres.2014.03.042.

[3] J. Tao, J. Gao, L. Zhang, R. Zhang, H. Che, Z. Zhang, Z. Lin, J. Jing, J. Cao, S. C. Hsu, (2014). $PM_{2.5}$ pollution in a megacity of southwest China: source apportionment and implication, Atmospheric Chemistry and Physics, 14 8679-8699. doi: 10.5194/acp-14-8679-2014.

[4] M. Cao, W. Li, P. Ge, M. Chen, J. Wang, (2022). Seasonal variations and potential sources of biomass burning tracers in particulate matter in Nanjing aerosols during 2017-2018, Chemosphere, 303. 135015. doi: 10.1016/j.chemosphere.2022.135015.

[5] M. Zhou, L. Qiao, S. Zhu, L. Li, S. Lou, H. Wang, Q. Wang, S. Tao, C. Huang, C. Chen, (2016). Chemical characteristics of fine particles and their impact on visibility impairment in Shanghai based on a 1-year period observation, Journal of Environmental Sciences, 48, 151-160. doi: 10.1016/j.jes.2016.01.022.

[6] K. F. Ho, G. Engling, S. S. H. Ho, R. Huang, S. Lai, J. Cao, S. C. Lee,(2014). Seasonal variations of anhydrosugars in $PM_{2.5}$ in the Pearl River Delta Region, China, Tellus Series B-Chemical and Physical Meteorology, 66. doi: 10.3402/tellusb.v66.22577.

[7] J. Wang, X. Ge, Y. Chen, Y. Shen, Q. Zhang, Y. Sun, J. Xu, S. Ge, H. Yu, M. Chen, (2016). Highly time-resolved urban aerosol characteristics during springtime in Yangtze River Delta, China: insights from soot particle aerosol mass spectrometry, Atmospheric Chemistry and Physics, 16, 9109-9127. doi: 10.5194/acp-16-9109-2016.

[8] B. J. Turpin, P. Saxena, E. Andrews, (2000). Measuring and simulating particulate organics in the atmosphere: problems and prospects, Atmospheric Environment, 34, 2983-3013. doi: 10.1016/S1352-2310(99)00501-4.

[9] N. Zheng, S. Song, X. Jin, H. Jia, Y. Wang, Y. Ji, L. Guo, P. Li, (2019). Assessment of Carbonaceous Aerosols at Mount Tai, North China: Secondary Formation and Regional Source Analysis, Aerosol and Air Quality Research, 19, 1708-1720. doi: 10.4209/aaqr.2019.06.0316.

[10] G. Wang, S. Cheng, J. Li, J. Lang, W. Wen, X. Yang, L. Tian, (2015). Source apportionment and seasonal variation of PM2.5 carbonaceous aerosol in the Beijing-Tianjin-Hebei Region of China, Environmental Monitoring and Assessment, 187. doi: 10.1007/s10661-015-4288-x.

[11] T. Nguyen Thi Thu, D. Nghiem Trung, K. Sekiguchi, T. Ly Bich, H. Nguyen Thi Thu, R. Yamaguchi, (2018). Mass Concentrations and Carbonaceous Compositions of $PM_{0.1}$, $PM_{2.5}$, and PM_{10} at Urban Locations in Hanoi, Vietnam, Aerosol and Air Quality Research, 18, 1591-1605. doi: 10.1007/s10661-015-4288-x.

[12] J. Plaza, B. Artinano, P. Salvador, F. J. Gomez-Moreno, M. Pujadas, C. A. Pio, (2011). Short-term secondary organic carbon estimations with a modified OC/EC primary ratio method at a suburban site in Madrid (Spain), Atmospheric Environment, 45, 2496-2506. doi: 10.1016/j.atmosenv.2011.02.037.

[13] O. Ramirez, A. M. Sanchez de la campa, J. de la Rosa, (2018). Characteristics and temporal variations of organic and elemental carbon aerosols in a high-altitude, tropical Latin American megacity, Atmospheric Research, 210, 110-122. doi: 10.1016/j.atmosres.2018.04.006.

[14] Q. Zhao, S. Qin, C. Zhao, Y. Sun, B. Panchal, X. Chang, (2021). Origin and geological implications of super high sulfur-containing polycyclic aromatic compounds in high-sulfur coal, Gondwana Research, 96219-231. doi: 10.1016/j.gr.2021.04.012.

[15] C. E. Tshehla, C. Y. Wright, (2019). Spatial and Temporal Variation of PM_{10} from Industrial Point Sources in a Rural Area in Limpopo, South Africa, International Journal of Environmental Research and Public Health, 16. doi: 10.3390/ijerph16183455.

[16] F. Xue, H. Niu, S. Hu, C. Wu, C. Zhang, N. Gao, X. Ren, S. Li, W. Hu, J. Wang, J. Fan, (2022). Seasonal variations and source apportionment of carbonaceous aerosol in $PM_{2.5}$ from a coal mining city in the North China Plain, Energy Exploration & Exploitation, 40, 834-851. doi: 10.1177/01445987211043211.

[17] G. Hu, Y. Zhang, J. Sun, L. Zhang, X. Shen, W. Lin, Y. Yang, (2014). Variability, formation and acidity of water-soluble ions in $PM_{2.5}$ in Beijing based on the semi-continuous observations, Atmospheric Research, 145, 1-11. doi: 10.1016/j.atmosres.2014.03.014.

[18] B. Wang, Z. Tang, N. Cai, H. Niu, (2021). The characteristics and sources apportionment of water-soluble ions of $PM_{2.5}$ in suburb Tangshan, China, Urban Climate, 35, 100742. doi: 10.1016/j.uclim.2020.100742.

[19] X. Zhang, X. Zhao, G. Ji, R. Ying, Y. Shan, Y. Lin, (2019). Seasonal variations and source apportionment of water-soluble inorganic ions in $PM_{2.5}$ in Nanjing, a megacity in southeastern China, Journal of Atmospheric Chemistry, 76, 73-88. doi: 10.1007/s10874-019-09388-z.

[20] D. Yue, M. Hu, Z. Wu, Z. Wang, S. Guo, B. Wehner, A. Nowak, P. Achtert, A. Wiedensohler, J. Jung, Y. J. Kim, S. Liu, (2009). Characteristics of aerosol size distributions and new particle formation in the summer in Beijing, Journal of Geophysical Research-Atmospheres, 114. doi: 10.1029/2008JD010894.

[21] A. Charron, L. Polo-Rehn, J.-L. Besombes, B. Golly, C. Buisson, H. Chanut, N. Marchand, G. Guillaud, J.-L. Jaffrezo, (2019). Identification and quantification of particulate tracers of exhaust and non-exhaust vehicle emissions, Atmospheric Chemistry and Physics, 19, 5187-5207. doi: 10.5194/acp-19-5187-2019.

[22] F. Wang, Z. Guo, T. Lin, N. L. Rose, (2016). Seasonal variation of carbonaceous pollutants in $PM_{2.5}$ at an urban 'supersite' in Shanghai, China, Chemosphere, 146, 238-244. doi: 10.1016/j.chemosphere.2015.12.036.

[23] J. Ding, W. Huang, J. Zhao, L. Li, G. Xiong, C. Jiang, D. Ye, D. Li, J. Wang, J. Yu, R. Liu, (2022). Characteristics and source origins of carbonaceous aerosol in fine particulate matter in a megacity, Sichuan Basin, southwestern China, Atmospheric Pollution Research, 13, 101266. doi: 10.1016/j.apr.2021.101266.

[24] J.-K. Choi, J.-B. Heo, S.-J. Ban, S.-M. Yi, K.-D. Zoh, (2012). Chemical characteristics of $PM_{2.5}$ aerosol in Incheon, Korea, Atmospheric Environment, 60, 583-592. doi: 10.1016/j.atmosenv.2012.06.078.

[25] Z. Niu, F. Zhang, J. Chen, L. Yin, S. Wang, L. Xu, (2013). Carbonaceous species in $PM_{2.5}$ in the coastal urban agglomeration in the Western Taiwan Strait Region, China, Atmospheric Research, 122 102-110. doi: 10.1016/j.atmosres.2012.11.002.

[26] J. Duan, J. Tan, D. Cheng, X. Bi, W. Deng, G. Sheng, J. Fu, M. H. Wong, (2007). Sources and characteristics of carbonaceous aerosol in two largest cities in Pearl River Delta Region, China, Atmospheric Environment, 41, 2895-2903. doi: 10.1016/j.atmosenv.2006.12.017.

[27] L. Zhang, Y. Huang, Y. Liu, F. Yang, G. Lan, C. Fu, J. Wang, (2015). Characteristics of Carbonaceous Species in $PM_{2.5}$ in Wanzhou in the Hinterland of the Three Gorges Reservoir of Northeast Chongqing, China, Atmosphere, 6, 534-546. doi: 10.3390/atmos6040534.

[28] L. M. Castro, C. A. Pio, R. M. Harrison, D. Smith, (1999). Carbonaceous aerosol in urban and rural European atmospheres: estimation of secondary organic carbon concentrations, Atmospheric Environment, 33, 2771-2781. doi: 10.1016/S1352-2310(98)00331-8.

[29] R. Arimoto, R. A. Duce, D. L. Savoie, J. M. Prospero, R. Talbot, J. D. Cullen, U. Tomza, N. F. Lewis, B. J. Ray, (1996). Relationships among aerosol constituents from Asia and the North Pacific during PEM-West A, Journal of Geophysical Research, 101. doi: 10.1029/95JD01071.